Measurement of distortion product phase in the ear canal of the cat

P. F. Fahey
Department of Physics, University of Scranton, Scranton, Pennsylvania 18510

Jont B. Allen
AT&T Labs, Florham Park, New Jersey 07932

(Received 11 October 1996; revised 25 June 1997; accepted 26 June 1997)

Amplitudes of odd order distortion products (DPs) that are detected in animal ear canals have been used to probe cochlear health, to search for cochlear amplification, and to measure aspects of cochlear mechanical frequency response. Like the DP amplitude, DP phase is also an important measure of the cochlear mechanical response. Reported here are measurements of DP phase in the ear canal of the cat. The phase data show frequency-dependent time delays. One of these delays is a function of f_2, the frequency of the higher-frequency primary. Hence the DP phase ϕ_d is of the form $\phi_d=\phi_0+\omega_d\tau$, where ω_d is the DP angular frequency and τ is a fixed time delay. Our results show that ϕ_d is independent of input level a_2 as long as the ratio $a_2/a_1\leqslant 2$, where a_2 and a_1 are the amplitudes of the input tones. As a_2/a_1 becomes greater than two, the fixed time delays increase for DPs whose frequencies are less than the frequencies of the input tones. When both levels are varied together the delay increases as the levels decrease. There can be phase changes as large as π associated with deep nulls in the DP magnitude for the two lower-frequency DPs. Features of the nulls may be modeled assuming that there is partial reflection of the DP wave from the DP place. The assumption of energy reemitted from the DP place also explains amplitude-ratio-dependent time delays and 2π level-dependent bifurcations in phase. The DP phase shows different dependencies for $f_2<1$ kHz compared to $f_2>2$ kHz. © *1997 Acoustical Society of America.* [S0001-4966(97)02111-5]

PACS numbers: 43.64.Kc, 43.64.Bt, 43.64.Jb [RDF]

INTRODUCTION

Intermodulation distortion products (DPs) that are generated by the nonlinear mechanical response of the inner ear to an input of two primary tones are detectable in the ear canal. Since mammals, birds, and reptiles have nonlinear inner ears and, since DPs generally show good signal to noise ratios, DPs can be a useful noninvasive probe of the mechanical response of the cochlea. Indeed, attempts have been made to use DPs as an objective measure of hearing integrity in humans (measurement issues summarized in Whitehead *et al.*, 1994); as a probe of cochlear amplification (Allen and Fahey, 1992); and as a probe of the cochlear frequency response (Brown and Gaskill, 1990; Brown *et al.*, 1992; Allen and Fahey, 1993). Reported here are measurements in cat of the phase of the odd order DPs at frequency f_d equal to $2f_1-f_2$, $3f_1-2f_2$, $2f_2-f_1$, and $3f_2-2f_1$ (f_1 is the frequency of the lower-frequency primary whose respective amplitude is a_1 and f_2 is the frequency of the higher-frequency primary whose respective amplitude is a_2).

Frequencies of the odd order DPs are given by the general expression $f_d=f_1+n(f_2-f_1)=f_1+n\Delta f$, where n is either a positive or a negative integer. If $n\geqslant 2$, the DPs have frequencies greater than either of the primary frequencies and if $n\leqslant -1$ the DP frequency is less than either of the primary frequencies. (When $n=0$, 1 the equation above evaluates to one of the primary frequencies.) Because, when reading the text, it is easy to confuse $f_d=2f_1-f_2$ and $f_d=2f_2-f_1$, we will use the following notation throughout the text. $f_d(-2)=f_1-2\Delta f=3f_1-2f_2$, $f_d(-1)=f_1-\Delta f=2f_1-f2$, $f_d(+2)=f_1+2\Delta f=2f_2-f_1$, and $f_d(+3)=3f_2-2f_1$. $f_d(-1)$ and $f_d(+2)$ are said to be third order or cubic DPs and $f_d(-2)$ and $f_d(+3)$ are said to be fifth order. In a power series expansion, third-order DPs are generated by any odd power in the expansion that is cubic or greater. Fifth-order DPs are generated by any odd power in the expansion that is fifth order or greater. The notation that we suggest identifies the DPs as though they are components in a spectrum centered about the primaries. A negative number in the parentheses means the DP is lower frequency than the primaries and a positive number in the parentheses means that the DP has a higher frequency than either primary. The number in the parentheses is the same as the coefficient of f_2 in the DP.

I. DISTORTION PRODUCT MEASUREMENT

A. Animal preparation and sound system

Both the sound system and the animal preparations in this study were essentially the same as in Allen (1983), except that there was no surgery to expose the auditory nerve. The animals were anesthetized with sodium pentobarbitol and the bulla and septum were open. Enough of the ear canal was removed to allow positioning of the probe microphone to within a few millimeters of the tympanic membrane. Input tone bursts of 40-ms duration and 50% duty cycle were digitally synthesized. The DP phase is the fast Fourier transform (FFT) phase of the time response waveform built from ten

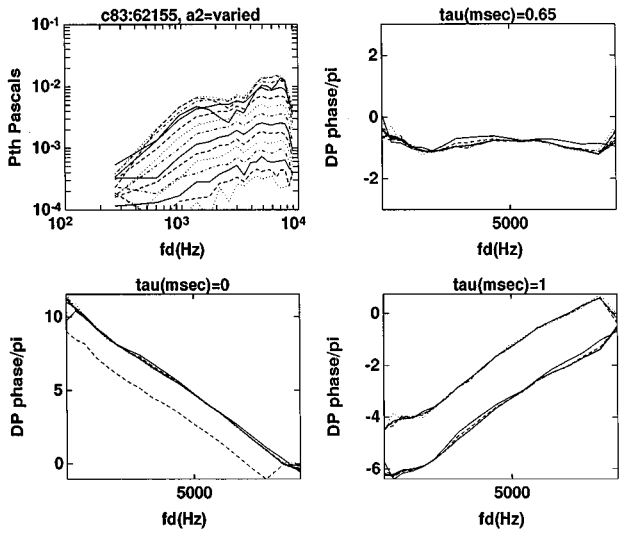

FIG. 1. The top left panel shows the magnitude of the $f_d(-1)=2f_1-f_2$ DP as a function of DP frequency for constant $f_2=9$ kHz. Each magnitude curve was measured at a level wherein a_2 was decreased by 3 dB from the previous curve while a_1 was held constant at 1.0 Pa (1.0 Pa is 94 dB SPL). The DP amplitude was maximum when the value of a_2 was 6 dB less than the value of a_1. The value of the phase was independent of the level of a_2 for $52 \leqslant a_2 \leqslant 85$ dB SPL. The bottom left panel shows the phase of the DP as a function of DP frequency for no subtracted fixed time delay. In the top right panel the phase is plotted after a fixed time delay of 0.65 ms has been subtracted and in the bottom right panel phase is plotted after subtracting a fixed delay of 1.0 ms. It is evident that a fixed delay of 0.65 ms does the best job of making the phase independent of frequency. The frequency axis in the magnitude plot is logarithmic while the frequency axes in the phase plots are linear.

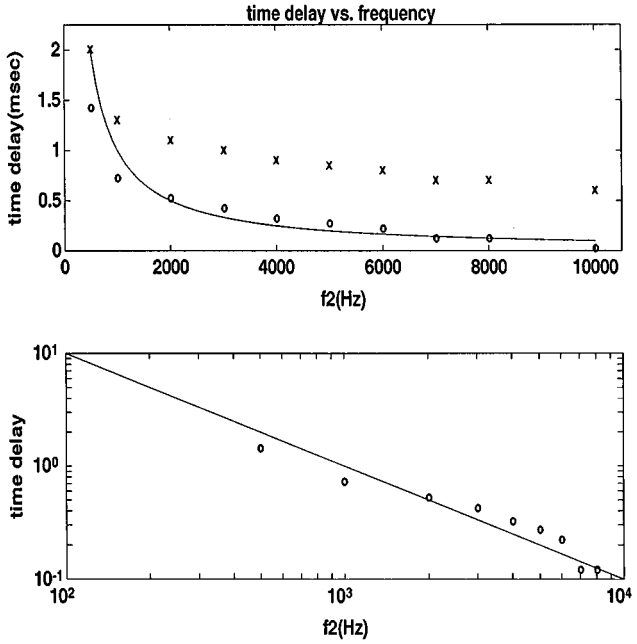

FIG. 2. The top plot shows the values of the fixed time delays τ plotted versus f_2, symbolized by $\times$'s; $\tau-0.6\,\text{ms}=\Delta\tau$ is represented by the $\bigcirc$'s; and the curve is a plot of $1/f_2$ vs f_2. A reasonable first approximation to $\Delta\tau$ is $1/f_2$ as shown by the solid curve. The bottom plot shows the logarithm of $\Delta\tau$ versus the logarithm of frequency. The $\bigcirc$'s are the data and the solid line is $1/f_2$.

averages of the response. For the distortion products reported here the response was not sensitive to the tone burst windowing, whether Kaiser, raised cosine, or none. The data are typical across more than a dozen animals.

B. The measurement

For each animal studied, both the sound delivery system impedance Z_0 and the input impedance of the animal preparation Z_{in} were measured after Allen (1986) and Voss and Allen (1994). The DP pressure measured in the ear canal P_{ec} was expressed as a Thevenin equivalent source pressure P_{Th} given by $P_{\text{Th}}=P_{\text{ec}}(1+Z_{\text{in}}/Z_0)$ (Fahey and Allen, 1986, 1988). Since DP volume velocity in the ear canal due to the DP pressure source in the cochlea depends upon the value of the transducer impedance, the use of the Thevenin equivalent pressure reduces the experimental variations of the results due to the transducer impedance. For most of the data presented here for $0.8\,\text{kHz}<f_2<8\,\text{kHz}$, $P_{\text{Th}}\approx 2P_{\text{ec}}$ since $Z_0 \approx Z_{\text{in}}$. Therefore while the measurements presented here are of P_{Th} phase, they are similar to raw P_{ec} phase. The magnitude and phase of the DPs were measured by taking the FFT of the time waveform of the ear canal pressure. Since the phase has an uncertainty of 2π, when plotting phase versus frequency, the phase data was unwrapped so that change in the phase from one point to the next was minimized. By first subtracting that part of the phase that is due to a fixed time delay we eliminate much of the potential for uncertainty in the phase unwrapping. In the data that follows it will occasionally be useful to keep this uncertainty in mind when viewing some of the features in the plotted phases. Stover *et al.* (1996) used DP magnitude and phase to define a ''filter function'' and its inverse Fourier transform that was called the ''IFFT waveform.'' We will refer to these constructions as the FILTF and WAVEF. We constructed FILTF's by inserting a 128 point spline fit of the data into a spectrum that was padded with zeroes both at frequencies below the lowest value of f_d and at frequencies above the highest value of f_d. A 1024 point WAVEF was generated from the FILTF inverse Fourier transform. The functional shape of the WAVEF resembles a system impulse response, but the WAVEF is not a system impulse response because it is nonlinear in origin. The WAVEF is a different way of presenting the same data as the DP magnitude and phase data. The advantage of the WAVEF presentation of the data is that delays that are implicit in the raw phase data are presented weighted by the energy at the various delays. This technique

TABLE I. Fixed time delay as a function of f_2.

f_2 (kHz)	0.5	1.0	2.0	3.0	4.0	5.0	6.0	7.0	8.0	10.0	12.0	17.0
τ (ms)	2.0	1.3	1.1	1.0	0.9	0.85	0.8	0.7	0.7	0.60	0.60	0.60
$\Delta\tau=\tau-0.6$	1.4	0.7	0.5	0.4	0.3	0.25	0.2	0.1	0.1	⋯	⋯	⋯
$f_2\Delta\tau$	0.7	0.7	1.0	1.2	1.2	1.25	1.2	0.7	0.8	⋯	⋯	⋯

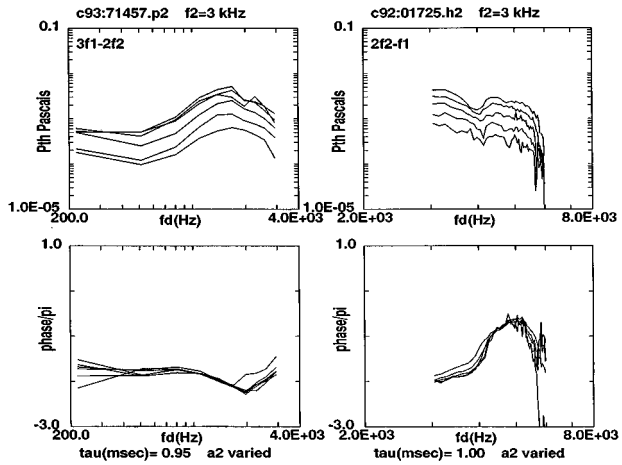

FIG. 3. In the left panels magnitude and phase are plotted as a function of f_d for the lower frequency fifth-order DP, $f_d(-2)=3f_1-2f_2$, as a_2 is decremented from $a_2=0.78$ Pa in 3-dB steps at a constant $a_1=0.77$ Pa. The lowest value of a_2 is 0.14 Pa. The phase changes little with a_2 if $a_2<0.5a_1$. In the right panels the higher-frequency third-order DP, $f_d(+2)=2f_2-f_1$, magnitude, and phase are plotted as functions of DP frequency. The value of $a_1=0.65$ Pa and $0.16\leqslant a_2\leqslant 0.65$ Pa.

is conceptually more mathematically simple than the method of Brown *et al.* (1996) and it has the added potential of giving more information about signal delays.

C. Data presentation

Figure 1 displays the effects of subtracting a fixed time delay from the phase data and Fig. 2 is a plot of Table I. Then Figs. 3–8 have the same presentation format. Each is a plot of the ear canal Thevenin equivalent DP pressure plotted against the DP frequency f_d. Each curve is measured at a different level of the input. At the top of the figure are listed the animal and file and the constant value of f_2. At the bottom of the figure are the value of the fixed time delay τ in ms. That part of the phase that is due to the fixed time delay

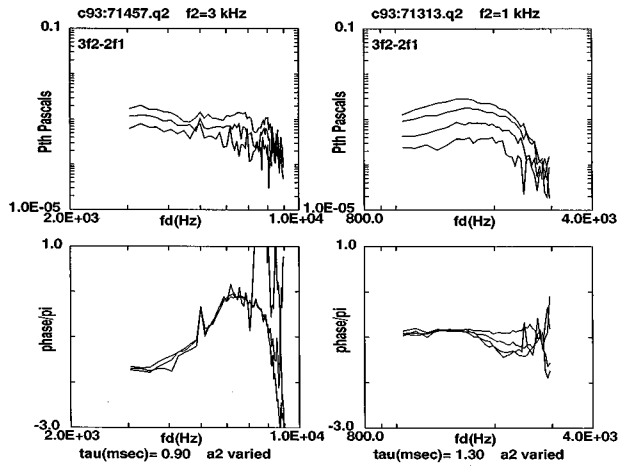

FIG. 4. The higher-frequency fifth-order DP, $f_d(+3)$, magnitude, and phase are plotted as functions of DP frequency. a_2 is decremented in 3-dB steps. In the left panels the phase is independent of a_2 for $0.39\leqslant a_2\leqslant 0.78$ Pa while $a_1=0.77$ Pa. In the last curve the data above $f_d=7$ kHz is in the noise. In the right panel, starting at $a_2=0.38$ Pa, a_2 is decremented in 3-dB steps to a final value of $a_2=0.13$ Pa while a_1 is constant at 0.37 Pa. The phase changes little with a_2 when $1<f_d<1.7$ kHz.

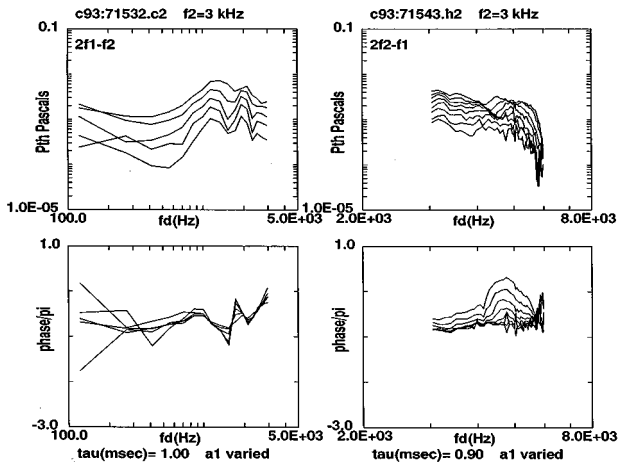

FIG. 5. In the left panels magnitude and phase are plotted as functions of f_d for the lower-frequency third-order DP, $f_d(-1)$, as a_1 is decremented in 3-dB steps from $a_1=0.63$ Pa to $a_1=0.15$ Pa at a constant $a_2=0.63$ Pa. The phase changes little with a_1 except in the vicinity of the nulls in the magnitude between 1.5 and 2.5 kHz. In the right panels magnitude and phase are plotted as a function of f_d for the higher-frequency third-order DP, $f_d(+2)$, as a_1 is decremented in 3-dB steps from $a_1=0.75$ Pa to $a_1=0.067$ Pa at a constant $a_2=0.78$ Pa. The lowest four phase curves are independent of a_1 level.

$\omega_d\tau$ has been subtracted from the phase that is plotted. Therefore given that $\phi_d=\phi_0+\omega_d\tau$, the phase that is plotted is ϕ_0. Also identified at the bottom of the plot is the level that was varied. The data in this study are at fixed values of f_2. Here, f_d is varied by changing the value of f_1.

The input levels used in this study were as high as 1.0 Pa (or 94 dB SPL) and were higher than levels generally used in human studies. Correspondingly, the DP levels were as high as 0.02 Pa (or 60 dB SPL).

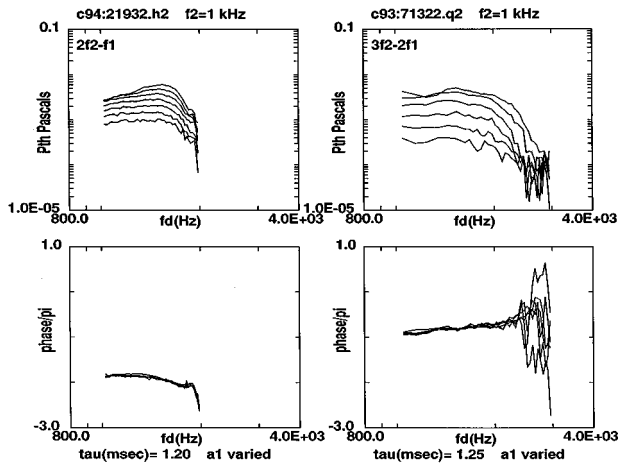

FIG. 6. In the left panels magnitude and phase are plotted as functions of f_d for the higher-frequency third-order DP, $f_d(+2)$, as a_1 is decremented in 3-dB steps starting at $a_1=0.73$ Pa and ending at $a_1=0.09$ Pa at a constant $a_2=0.74$ Pa. All seven phase curves superimpose. In the right panels magnitude and phase as functions of f_d are shown for the higher-frequency fifth-order DP, $f_d(+3)$, as a_1 is varied from $a_1=0.62$ Pa to $a_1=0.11$ Pa and a_2 is constant at 0.64 Pa. Notice that the phase does not depend on a_1 at this frequency of f_2. For $f_d>2.3$ kHz the magnitude is in the noise at the lower values of a_1; hence, the phase is noisy also. When $f_2\leqslant 1.0$ kHz the phases of the higher-frequency DPs seem to show less dependence on a_1 than at the higher f_2.

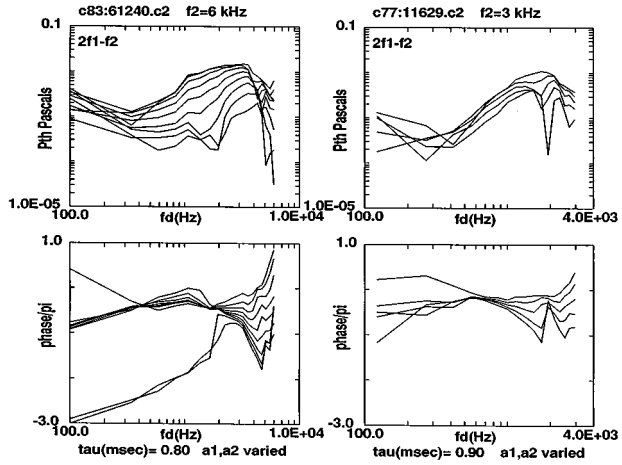

FIG. 7. Magnitude and phase are plotted as a function of f_d for the lower-frequency third-order DP, $f_d(-1)$, as a_1 and a_2 are decremented in 3-dB steps beginning at $a_1=a_2=0.95$ Pa and ending at $a_1=a_2=0.06$ Pa in the left panel and from 1.0 to 0.26 Pa in the right panel. In the left panels at a value of f_d just less than 2 kHz the phase seems to be independent of level (except for the phase curves measured at the two lowest levels). For higher frequencies than this fixed phase point the phase appears as though it rotates about this point in a clockwise direction, i.e., the slope of the phase becomes more negative as the level decreases. At frequencies less than the fixed point the phase varies slightly with decreasing level. For the two phase curves at the two lowest input levels a π phase shift occurs at about this frequency. Comparing the two lowest input level phase curves with the higher level curves shows that there is a level-dependent phase bifurcation of 2π for $f_d<2$ kHz. In the right panels, while there is not a fixed phase point as in the previous figure, the phase varies little around $f_d=0.7$ kHz. In this figure, at the lowest level of the primaries a sharp null is evident in the magnitude at $f_d=2$ kHz. There is also a π phase shift at this frequency.

II. RESULTS

A. Time delays

In Fig. 1 the ear canal Thevenin equivalent pressure magnitude of a $f_d(-1)=2f_1-f_2$ DP is plotted versus its own frequency in the top left panel; the phase versus frequency with no fixed delay subtracted is plotted in the bottom left panel; in the top right panel a fixed time delay of 0.65 ms has been subtracted from the phase; and, in the bottom right panel a fixed delay of 1.0 ms has been subtracted. Here $f_2=9$ kHz and the subtracted time delay of 0.65 ms removes most of the phase variation at low frequencies (and, in this file, also at high frequencies).

The modeling results of Matthews and Molnar (1986) show that most of the DP energy is generated in the vicinity of the f_2 place. There are also good general theoretical reasons that DPs generated by a saturating nonlinearity would be generated near the f_2 places. The maximum DP is generated when the levels of the two inputs to the nonlinearity are approximately equal. For cochlear excitations that region is near the f_2 place. The data presented in this study are at constant f_2.

In Table I we tabulate the values of the fixed time delay as a function of f_2 under the condition that one of the primary levels was constant and the other primary level was varied. For the $f_d(-1)$ and $f_d(-2)$ DPs a further condition is that $a_2/a_1\leqslant 2$. Under these conditions the phase is independent of the level of the varied primary and the low-frequency slope of the phase as a function of $\omega_d(=2\pi f_d)$ is constant; therefore, τ is constant. As f_2 increases the time delay decreases. These values are a good representation of the fixed time delay across the dozen animals used in this study and across the four DPs. For higher values of f_2 the time delays come primarily from $f_d(-1)$ and $f_d(-2)$ data records. At values of f_2 on the order of 10 kHz or greater, the fixed time delay reaches an asymptote of about 0.6 ms. The third line of Table I shows the values of the time delays with the value of the asymptotic delay subtracted and the fourth line shows the values in the third line multiplied by their respective f_2. This product is of order one, suggesting that the time delays after the asymptotic delay has been subtracted is, to a first approximation, equal to $1/f_2$. A graph of the results in the table is Fig. 2.

When a_2/a_1 is greater than about two or three, the measured time delays for the $f_d(-1)$ and the $f_d(-2)$ DPs can be greater than the values in Table I. The increase ranged from 1.0 ms at lower values of f_2 to 0.3 ms at the highest values. The effect of the ratio a_2/a_1 is clearly seen in Fig. 9 and will be discussed in a following section. The longer delays could well be due to an increase in energy that arrives later because it has been reflected from the DP place.

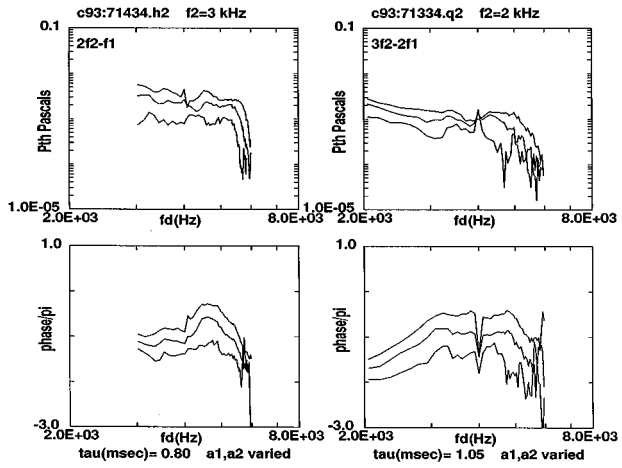

FIG. 8. a_1 and a_2 are decremented together by 3 dB each for the $f_d(+2)$ DP in the left panels and for the $f_d(+3)$ DP in the right panels. For both of these DPs the ratio $a_2/a_1=1.0$ and the initial values are $a_1=a_2=0.7$ Pa and the final values are 0.35 Pa. The sharp null in the phase at $f_d=4$ kHz in the right panels is probably due to mixing with the $2f_1+f_2$ DP which moves down in frequency as $f_d(+3)$ moves up (with decreasing f_1).

B. Phase dependence on primary level(s)

1. a_1 constant, a_2 varied

Figures 1, 3, and 4 show both DP magnitude and phase as a_1 is held constant and a_2 is decremented in 3-dB steps. In Fig. 1 the $f_d(-1)$ DP phase data shows that, except for the data acquired at the four highest levels of a_2, the phase curves are independent of level. In Fig. 3 (left) the same general independence of phase with level is shown for the $f_d(-2)$ DP. Phase as a function of a_2 and f_d is is shown in Fig. 3 (right) for the $f_d(+2)$ DP and again there is independence of a_2. Figure 4 (left) illustrates the independence of phase with a_2 level for the $f_d(+3)$ DP. This behavior is typical for $f_2\geqslant 2.0$ kHz. However, Fig. 4 (right) shows that

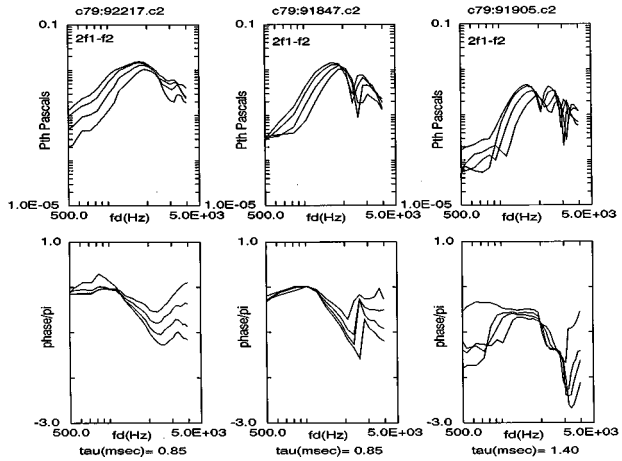

FIG. 9. In this figure a_1 and a_2 are decremented together in 3-dB steps while the ratio a_2/a_1 changes from 0.3 in the left panels to 1.0 in the middle panels to 3.0 in the right panels. The density of nulls increases as the ratio a_2/a_1 increases. In the left panel $0.31 \leqslant a_1 \leqslant 0.89$ Pa and $0.09 \leqslant a_2 \leqslant 0.34$ Pa. In the middle panel $0.22 \leqslant a_1 = a_2 \leqslant 0.61$ Pa. In the right panel $0.11 \leqslant a_1 \leqslant 0.31$ Pa and $0.33 \leqslant a_2 \leqslant 0.92$ Pa.

for the $f_d(+3)$ DP when $f_2 \leqslant 1.0$ kHz there is some independence of phase with changing a_2, but only for f_d within an octave or so of f_2.

2. a_1 varied, a_2 constant

The marked independence of phase across the DP frequency range with changing a_2 is not generally as pronounced with changing a_1. Figure 5 (left) shows that, as a_1 is decreased by 3 dB, the phase changes in the vicinity of nulls in the $f_d(-1)$ DP magnitude versus frequency curve. Indeed, the amplitude peak to valley ratio of the nulls seems to increase as a_1 is decremented. We will show in a later figure that the presence of nulls increases as the a_2/a_1 ratio increases.

For the $f_d(+2)$ DP when $f_2 \geqslant 2.0$ kHz we observe that the phase is independent of a_1 only at the lowest levels [as seen in Fig. 5 (right)]. This is also seen in the $f_d(+3)$ data. When $f_2 \leqslant 1.0$ kHz, the phase of the $f_d(+2)$ DP is generally independent of a_1 as is shown in Fig. 6 (left). Likewise, when the DP is $f_d(+3)$ and $f_2 \leqslant 1.0$ kHz, we also observe independence of phase with a_1 as shown in Fig. 6 (right).

Comparing the data of this and the previous section with the data of the next section, it is evident that phase changes much less when only one primary level is varied than when both primary levels are varied together.

C. Both a_1 and a_2 decreased

Figure 7 shows $f_d(-1)$ DP phases and magnitudes as both a_1 and a_2 are each decremented by 3 dB. Qualitatively, the same phase dependence on level is observed in the $f_d(-2)$ phase (e.g., see phase in Fig. 12). In Fig. 7, at $f_d \approx 2$ kHz (except for the two phase curves measured at the two lowest levels) the phase seems to be almost independent of input level and, as the levels decrease, the phase above $f_d = 2$ kHz decreases in a regular way. This pattern is commonly observed when changing a_1 and a_2 together. When f_d is greater than the value of f_d where the magnitude is maximum, $f_d^{\max}$, the phase decreases when both levels are decremented together. It is also observed that, as a_1 and a_2 are decremented together, the frequencies at which the sharp nulls occur in the DP magnitude increase. For the two higher-frequency DPs the change in phase with the decrease of both levels seems to be a simple decrease in phase as seen in the panels of Fig. 8.

D. Sharp nulls

In Fig. 7 (right panel) there is an example of a sharp null in the DP magnitude at $f_d = 2$ kHz. In the phase a shift of π radians is observed at the null. When nulls begin to form as the level is decreased, the phase always shows a discontinuity at the null frequency. For the deepest nulls the change in phase is π radians. The sharpness of the nulls and the sharpness of the π phase shift are indicative of wave interference.

The appearance of nulls in the data is a function of the ratio a_2/a_1. When $a_2/a_1 > 2$ the density of nulls is greater. Figure 9 illustrates this effect. In each set of panels both primaries are decremented together, while the ratio a_2/a_1 changes from 0.3 in the left panels to 1.0 in the middle panels to 3.0 in the right panels. The nulling is least when the ratio is least. When the data of Fig. 9 (right) is plotted on a linear frequency scale (not shown) it is evident that the frequency spacing between the nulls is approximately constant (possibly increasing slightly as f_d decreases). When both a_1 and a_2 are varied together the nulls shift toward higher values of f_d as the primary levels decrease.

III. DISCUSSION

A. Time delays

As previously mentioned, the fixed time delays in Table I were chosen to minimize the slope of the phase for $f_d \leqslant f_d^{\max}$. We also measured time delays by taking the negative of the slope of the complete phase versus linear angular frequency curve (Allen, 1983; Kimberley *et al.*, 1993; O Mahoney and Kemp, 1995) and, within the error of both techniques, measured the same values for delay. The correspondence of the two methods is clear from the phase plots of Fig. 1. The negative of the slope of the phase in the lower left-hand panel is equal to 0.65 ms. This is the delay that has been subtracted from the lower left panel phase in the plot of the upper right-hand panel.

Furthermore, following Stover *et al.* (1996) we built FILTF's from our data that we inverse Fourier transformed to get WAVEF's. As observed by them, the maximum of the magnitude of the WAVEF can be used to define a latency. The latencies found using this technique, with $a_2/a_1 < 1$, gave us the same values as shown in Table I, within the error of the techniques. Of course, this is to be expected from the mathematical properties of the inverse Fourier transform if, globally, the phase slope is approximately constant. The top panels of Fig. 10 show the WAVEF magnitudes for the same data as shown in Fig. 1 and in Fig. 5 (left). The peak in the magnitude occurs at times consistent with the values of the delay for $f_2 = 3$ kHz and $f_2 = 9$ kHz, respectively. The time delays in Table I characterize all of the animals used in this

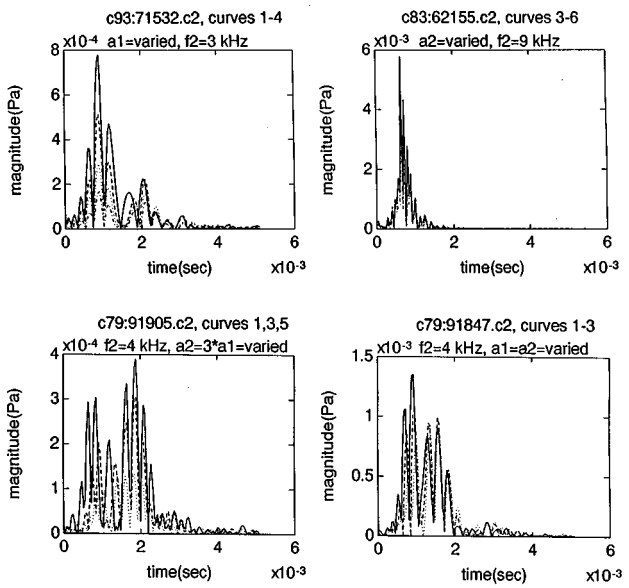

FIG. 10. WAVEF's constructed after Stover *et al.* (1996) have been constructed for some of the data in Fig. 5 (top left panel) and in Fig. 1 (top right panel). The magnitude of the responses is maximum at times that coincide with the delays determined by subtracting a fixed delay. The amplitudes of the impulse responses scale as expected from the curves in Fig. 5 (left) and Fig. 1. Notice that in the top left panel a second wave at a later time ($\approx$2 ms) grows relative to the first wave as a_1 decreases. The bottom panels of this figure show WAVEF magnitudes constructed from the data of the right and middle panels of Fig. 9. In the bottom left panel of this figure are the data taken when $a2/a1=3.0$ and in the bottom right panel when $a2/a1=1.0$. In the bottom left panel the amplitude of the later peak in the magnitude is larger than at the earlier peak. This is why the fixed delay as seen in Fig. 9 (right) is greater than in the Fig. 9 left or middle phase panels.

study. The values in Table I apply to every animal that we studied to within ± 0.3 ms, except at the lowest value of f_2, where the range was ± 0.5 ms. Kimberley *et al.* (1993) have shown that the time delay (also called latency) in humans decreases as the level of both primaries are increased together. This is also apparent in the cat data of Figs. 7 and 9. For example, calculating the delay from the complete phase versus linear frequency curve for Fig. 7 (left), the slope increases by a factor of about 1.5 from the highest levels to lowest.

The delays published here for a cat are much smaller than the delays in a human in the same frequency range. In a human, when $f_2 \approx 4$ kHz, the latency is on the order of 3 to 4 ms (Brown *et al.*, 1992; Kimberley *et al.*, 1993; Whitehead *et al.*, 1996; Stover *et al.*, 1996). Stover *et al.* have observed that the latency for some other odd order DPs is the same as for the $f_d(-1)$ DP. The cat data in this study also suggests that the fixed time delay is independent of DP order. This is certainly not surprising if it is assumed that the various odd order DPs are generated by the same mechanism at the same place. Whitehead *et al.* (1996) directly measured the time to onset of the DP signal in the ear canal and found times consistent with the measurement of latency from the slope of the phase. Stover *et al.* (1996) have shown that the delays derived from the WAVEF are commensurate with latency determined by the slope of the phase. Hence the four methods used to measure delay all yield consistent results. The phase data that we show in this study has the fixed delay subtracted from the total phase so that we emphasize and magnify the other features in the phase data (i.e., the nulls and what is happening to the phase above $f_d = f_d^{\max}$).

When the DP delays are compared with neural delays (of inputs at $f=f_d$ at the f_2 place) in the same kind of animal preparation (Allen, 1983), the DP delays match up well with minimum values for neural delays (after subtracting out approximately 0.9 ms of synaptic delay. These delays also generally correspond to the latencies of neural onset to condensation clicks in a cat of Kim and Molnar (1979, Fig. 8), although for characteristic frequencies greater than 2.0 kHz their latencies are systematically smaller than our fixed time delays. Part of neural delay is due to one-way travel time. Initially, one might think that some of the DP delay as due to a two-way travel time (for fixed f_2), i.e., the travel time of f_1 to the f_2 place and the travel time out of the cochlea of the DP. However, the travel time of f_1 to the f_2 place changes little as f_1 decreases; hence, the DP phase delay is primarily due to travel time of the DP excitation to the ear canal. That the minimum neural delay and the DP delay are approximately the same as a function of frequency again suggests that the DP is generated primarily at the f_2 place.

In a human, there seems to be some question on whether the DP delay is a measure of two-way travel time or one-way travel time (Kimberley *et al.*, 1993; O Mahoney and Kemp, 1995; Bowman *et al.*, 1997). Assuming that human DP biophysics is the same as a cat's, and that the cat data show that neural travel time delay and DP delay are the same, it is clear that, for at least one DP component, the travel delay is due to one way travel time.

The relationship between fixed delay and f_2 is both what one would expect from models of cochlear macromechanics and from the theory of causal transfer functions. From Table I it is evident that there seems to be a minimum delay that is frequency independent and would be due to nonspecific delays such as measurement system delay (determined from the impulses response as derived from the wideband frequency response of the animal preparation) of between 0.2 and 0.3 ms and delay in communicating a signal from the base of the cochlea to the ear canal. This minimum delay is approximately 0.6 ms. If this value is subtracted from all of the other delay values and then the answer is multiplied by the respective f_2 for $1.0 \leqslant f_2 \leqslant 8.0$ kHz, this time-frequency product is a constant N of order 1 (specifically, $0.7 \leqslant N \leqslant 1.2$), showing that the low-frequency limit is basically proportional to $1/f_2$ (Fig. 2). The correlation of delay with f_2 can be expected if it is assumed that DP generation is at the f_2 place. For direct excitation of the cochlea, the proportionality of delay to $1/f_{\mathrm{CF}}$ (which is the same as f_2 in this context) for low-frequency excitation has been derived by Allen (1983) using the WKB-approximation cochlear model. Furthermore, using one of the relations between the real part and the imaginary part of a general transfer function (or a general immittance) derived by Bode (Bode, 1945, Chap. 13) it can be shown that the time delay in the low-frequency limit is inversely proportional to the resonant frequency (or the band-edge frequency for a low-pass system). The constant of proportionality depends only on the shape of the transfer function. (This relationship is easily seen in the expression for phase of a

damped simple harmonic oscillator where the constant of proportionality is the inverse of $2\pi Q$, where Q is the quality factor.) Assuming that the shape of the transfer function varies little with f_2; then, the proportionality of τ to $1/f_2$ would be expected.

B. The level dependence

Both the magnitude and phase curves show that there is much more regularity to the DP generation when only one input level is varied than when both levels are varied (e.g., Zwicker, 1981; Zwicker and Harris, 1990; Fahey and Allen, 1986, 1988; Whitehead *et al.*, 1995).

For the $f_d(-1)$ DP and the $f_d(-2)$ DP, when $a_2 < (a_1 = \text{const})$, the phase and the shape of the magnitude curve are invariant with respect to the value of a_2, as seen in the example of Fig. 1 and of Fig. 3 (left). Given that basilar membrane (BM) response changes shape (Rhode, 1980; Ruggero and Rich, 1991) with level, it could be expected that the DP generation could not be invariant with level. However, the conditions of the DP generation reported here, when thought of in terms of a two-tone suppression experiment where f_1 is a low-frequency suppressor at the f_2 place, could decrease the sensitivity of the most sensitive response region (or ''tip'') of the BM and/or the neural frequency tuning response at the f_2 place. The levels used were generally high, as the varied primary usually ranged between roughly 94 and 54 dB SPL. The primary that was not varied was usually fixed somewhere between 94 and 84 dB SPL. For the $f_d(-1)$ DP with a_2 varied the value of the fixed a_1 was in the range where it would suppress the a_2 response at its characteristic place. Basically, the most input sensitive region of the response would have been removed (Fahey and Allen, 1985; Ruggero *et al.*, 1992).

Given the measurements of magnitude and phase for the a_1 constant with $a_2/a_1 < 2$ for the two lower-frequency DPs, the data show that the DP generation process simply scales the DP magnitude with a_2 and that the frequency features of the DP are invariant under a_2 scaling.

When a_1 is varied with a_2 fixed, the phase is more dependent upon input level for the two lower-frequency DPs. In Fig. 5 (left) the phase varies around the frequencies where there are nulls in the the magnitude response curve. The phase change upon stepping through the null frequency gets greater as a_1 decreases. The WAVEF of the data of Fig. 5 (left panel) is shown in the top left panel of Fig. 10. The energy seems greatest at a time delay of ≈ 1 ms: however, there is also a second peak in the energy at ≈ 2 ms. As a_1 decreases (and the depth of the nulls increases) the peak in the energy at ≈ 2 ms increases relative to the peak at ≈ 1 ms. This same phase behavior is seen in the $f_d(-2)$ phase data (not shown). When a_1 only is varied, the nulls in the magnitude response do not change frequency.

For both the two higher-frequency DPs and for the lower-frequency DPs as long as $a_2/a_1 < 2$ phase is generally independent of the changing of one input level while the other input level is held constant.

C. Effect of the a_2/a_1 ratio as both levels are varied

In Fig. 9 we show that the presence of nulls depends upon the ratio a_2/a_1. When this ratio is large there are more nulls and/or the nulls are more evident. Also, from the values of the subtracted time delays given at the bottom of each phase panel, the time delay is largest at the largest value of the ratio. When both of the primary levels are varied together, the nulls in the magnitude of the $f_d(-1)$ and $f_d(-2)$ DPs shift to higher values of f_d as the levels decrease. The shifting of human DP nulls with level has been reported by He and Schmiedt (1993). They also show that the frequency spacing of nulls in a human is approximately 1/10 of an octave. In Fig. 9 (right), using both the magnitude and phase information it appears that there are nulls at $f_d = 1$, 2, and 3 kHz for an $f_2 = 4$ kHz. If the magnitude data in Fig. 9 (right) are replotted on a linear frequency scale (not shown), it is evident that the frequency spacing between the adjacent nulls is, roughly, constant.

WAVEF's of the data at $a_2/a_1 = 3$ and $a_2/a_1 = 1$ are shown in the bottom panels of Fig. 10. We find that the energy is more spread over time and peaks at later times as the a_2/a_1 ratio increases. Under some conditions the energy that arrives later can be greater than the energy that arrives earlier. The bottom panels of Fig. 10 also show that the time of the first peak increases as both of the primary levels decrease. This is consistent with the nulls moving to higher frequency with decreasing level and with the latency increasing as primary levels decrease (Kimberley *et al.*, 1993; Stover *et al.*, 1996; Whitehead *et al.*, 1996).

The relative growth of the later peaks to the early peak with decreasing both a_1 and a_2 that is evident in the WAVEF presented here for a cat was observed by Stover *et al.* (1996) in a human.

The number of nulls per Hz (the null density) in a human (He and Schmiedt, 1993) is much greater than the null density in a cat (this study). Another difference between the cat data and the human data is the level of the DPs. In He and Schmiedt the DP level is generally between -15 and 0 dB SPL, while the data of our Fig. 9 is around 30–40 dB SPL. The input levels in the human are also corresponding smaller. The noise floor in our measurements was dependent on frequency, but for $1\text{ kHz} < f_d < 8\text{ kHz}$ it was roughly a constant 10 dB SPL and we did measure DPs down to this level. At these lower levels (data not shown) we found no evidence that the null density would substantially increase as levels decrease. Even at the lowest levels, the null density was not much greater than 2 nulls per octave in a cat. Hence the null density difference between a human and a cat is not due to level differences. The ratio of the null density in the two species is roughly equal to the inverse of the ratio of the latencies. That the null spacing would be inversely proportional to the latency would suggest that propagation delays are implicated in the wave interference producing the nulls.

For a given pair of input levels, the nulls in human $f_d(-1)$ and $f_d(-2)$ data do not occur at the same f_d frequencies; however, the spacing between nulls (or peaks) is similar (Brown *et al.*, 1993b, Fig. 2). In a cat, it is also generally observed that the nulls of the two DPs do not occur at

the same value of f_d, nor do they occur at the same value of f_1.

The higher-frequency DPs, $f_d(+2)$ and $f_d(+3)$, do not show nulls like the two lower frequency DPs. At low levels of the DPs (20 dB SPL or less) we do occasionally observe nulls. However, these nulls are generally neither stable nor regular in frequency as input levels are decreased. The higher-frequency DPs do show predictable frequency-dependent features that are due to mixing with other components, such as the third harmonic of f_1 or the DPs at $2f_1+f_2$ or even $5f_1-2f_2$.

D. Source of the nulls

If it is assumed that the nulls are due to wave interference, then there are two or more waves mixing at the site of the microphone in the ear canal. If there are only two dominant waves, then, for a deep null the phase difference between the two waves of comparable amplitude must be $\approx\pi$. If there are several waves, then the phasor diagram must (almost) close. Waves of differing phases could be due to: (a) a path/time differences, such as path differences due to reflections; (b) a ''birefringence,'' i.e., two (or more) different values for wave velocity (e.g., Hubbard, 1993); or (c) two (or more) different nonlinear mechanisms with different phase at output.

The nulls observed psychophysically (i.e., within the cochlea) in the $f_d(-1)$ DP have been attributed by Zwicker (1981) to the interference of wavelets (i.e., waves from multiple sources).

Parallel approaches to modeling psychophysical DP nulls have been proposed to modeling ear canal DP nulls. Substantial discussion has been devoted in the literature to two possible mechanisms responsible for the microstructure observed in human DP emissions. The one proposed mechanism is the mixing of wavelets (Sun *et al.*, 1994; He and Schmiedt, 1996) and the other mixing due to energy reflected from the DP place (Talmadge *et al.*, 1996; Talmadge *et al.*, 1995; Brown *et al.*, 1996). If we assume that the nulls measured in a cat are due to the same physics as the microstructure measured in a human, then our cat data strongly support reflection from the DP place over distributed source generation of wavelets.

First, if the mixing of wavelets due to a distributed source of DP waves were the source of the nulls in the $f_d(-1)$ and the $f_d(-2)$ DPs, then one would also see nulls in the $f_d(+2)$ and $f_d(+3)$ DPs.

Second, as described below, using a simple semiempirical model, the assumption of reflection of energy from the DP place explains (a) several features of the nulls; (b) the commonly observed 2π phase splitting seen in DP data; and (c) the long delays in the $f_d(-1)$ and $f_d(-2)$ DP when a_2/a_1 is large.

There are several features of the nulls in our data that can be replicated with a simple physical picture. This picture assumes that the distortion product is generated at the f_2 place and that some of the DP wave is propagated basally (toward the stapes) and the remaining energy is propagated apically (toward the helicotrema). The time to propagate from the f_2 place to the stapes is assumed to be $1/f_2$ as the data in Table I would suggest. Waves that reach the stapes may be partially reflected and partially transmitted. The reflection coefficient at the stapes is r_{st}. Waves that propagate apically may be partially reflected at the DP place (Allen *et al.*, 1995). [This is essentially the same assumption that has been used by Zweig and Shera (1995) to explain the periodicity of evoked stimulus frequency emissions that are observed in the human ear canal.] The reflection coefficient at the DP place is r_{DP}. Two ways to model the phase change of the DP wave between the f_2 place and the DP place are to assume either a scaling symmetric cochlea, e.g., after Zweig and Shera (1995) or a nearly scaling symmetric cochlea, e.g., after Allen (1980). The scaling symmetric cochlea would have a phase change from the stapes to the characteristic place that scales as $\hat{\phi}\ \log(f_d)$. The Allen model can be shown to have a basilar membrane delay between the stapes and the characteristic place f_d that can be approximated by a constant divided by $(f_d/f_{\mathrm{ref}})^{\beta}$ or α/f_d^{β}, where α has units of time and f_d is now a relative frequency that is dimensionless. The model basilar membrane response data of Allen yield $\alpha\approx 0.3$ and $\beta\approx 0.8$. ($\beta=1$ would be a scaling symmetric cochlea.) The time for the DP wave to travel from the f_2 place to the DP place is assumed, to a first approximation, to be the time to travel from the stapes to the DP place, minus the time to travel from the f_2 place to the stapes, $1/f_2$. An interferometer with either a delay after the Allen model or a delay after the Zweig and Shera model produces interference nulls that have a frequency spacing that is similar to that of the data. For the scaling symmetric cochlea assumption, a value of $\hat{\phi}\approx 0.31$ produces interference patterns that look like the cat data. A picture of the interference pattern produced by the scaling symmetric cochlea assumption is shown in the top panel of Fig. 11 and the pattern produced by the Allen basilar membrane model is shown in the bottom panel of Fig. 11. To a first approximation the reflection coefficients are assumed to be independent of amplitude. Details of this physical picture will be published separately. With reflections at the stapes and at the DP place there will be an infinite sum of waves that mix at the detector in the ear canal. The phase differences of the various waves that mix at the detector will depend upon the different travel times and upon any phase changes at reflection. The amplitude differences of the wavelets will depend upon the magnitudes of the reflection coefficients (we will assume that there is no significant attenuation on the basilar membrane). Letting r_{st} become zero, the above picture becomes a simple two-source model. The major consequence of $r_{st}\neq 0$ is to the sharpen the nulls and to broaden the maxima of the interference patters. As r_{st} is allowed to increase, one generates the sharp interfence patterns commonly pictured in optics textbooks (Born and Wolf, 1975, Sec. 7.6).

Our data are consistent with values of $r_{st}\leqslant 0.3$. The null density depends upon travel time assumptions and would be different for a human than for a cat. Indeed, as O Mahoney and Kemp (1995) have pointed out, ''In humans ears tone-burst-evoked emissions commonly have ten or more waves of delay.'' An examination of the data in the paper by Kimberley *et al.* (1993) shows a delay of between six and seven waves in human. Our data in Table I show that cats have one

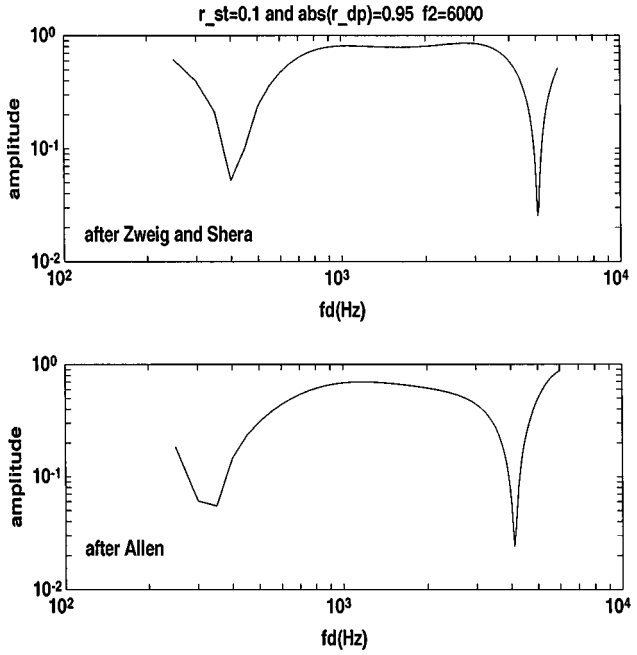

FIG. 11. The top panel shows the pattern of nulls calculated assuming a phase change from the stapes to the characteristic place of a scaling symmetric cochlea after Zweig and Shera (1995). The bottom panel shows the pattern of the nulls assuming the delays from the basilar membrane model of Allen (1980). For each panel, it was assumed that the time for a DP wave to travel from the f_2 place to the stapes was $1/f_2$. The values assumed for r_{st} and r_{DP} are shown at the top of the figure. r_{DP} is complex and its phase was adjusted between the top and the bottom panels in order to position the nulls at convenient values of f_d for the purpose of illustration. In this figure f_2 is assumed to be constant. Similar patterns are produced assuming that f_1 is constant or that f_2/f_1 is constant.

wave of delay. Hence the frequency spacing of such an interference pattern as described above in a human would be somewhere around one-tenth to one-fifth of the cat frequency spacing or from 0.1 to 0.2 kHz. Values of the observed frequency spacing in a human (He and Schmiedt, 1993; Brown *et al.*, 1993a; Piskorski *et al.*, 1995) are in this range.

The null density will depend upon the rate that the phases of the interfering waves changes as the f_d changes. Using the model described above, during a frequency sweep of f_d, we find a maximum of three nulls. This maximum is only slightly dependent on the starting value of f_2. The relative independence on the starting value of f_2 on the maximum number of nulls per f_d sweep is also a feature of the data. The null density in both the model and the data (Piskorski *et al.*, 1995) is the same if f_2 is held constant, if f_1 is held constant, or if the ratio f_1/f_2 is held constant.

How is it possible that more energy arrives later than the energy that goes directly from the source to the detector? There are at least three possible explanations. First, if from the source one-half of the wave goes in each direction, and if the magnitude of $r_{\mathrm{DP}} \approx 1$, almost all of the energy of the original apically going wave eventually goes basally. Furthermore, if the magnitude of r_{st} is greater than zero, some of the original basally going wave gets delayed due to multiple reflections, then the energy that arrives after the first wave can be greater than the energy of the first wave.

Second, if from the source one half of the wave energy goes in each direction and if there is energy creation apical to the source, i.e., the effective $|r_{\mathrm{DP}}| > 1$, then, independently of the value of r_{st}, more energy will arrive later than earlier.

The third possibility that would allow more energy to arrive late than early assumes that, from the source, more energy is emitted apically than is emitted basally. If the impedance that the source sees in the apical direction is different than the impedance that the source sees in the basal direction, then the assumption that one-half of the energy goes in each direction would obviously be false.

Our data suggests that increasing the a_2/a_1 ratio might increase the energy emitted apically relative to that emitted basally. Both the $f_d(-1)$ and the $f_d(-2)$ show an increase in both delay and the presence of nulls as a_2/a_1 becomes greater than 2 or 3. Since this effect does not depend on the absolute values of the DPs [the $f_d(-2)$ DP is generally 10–15 dB less than the $f_d(-1)$ DP for the same level of primaries], the effect does not seem to be simply due to the nonlinearity of r_{DP}.

However, because it is a common observation that a null can occur for a particular value of the input levels at constant f_2, f_1, f_d, and a_2/a_1 when both levels are varied together, the ratio of a_2/a_1 is not the only factor that determines the energy returned from the DP place. To be able to explain all of the details of the generation of nulls one would have to know the level dependence of the reflection coefficient r_{DP}. The interference pattern seen in stimulus frequency emissions disappears with increasing level, suggesting that the effective reflection coefficient at the emission site decreases as the level increases. Other studies imply that the cochlear reflection coefficient increases with decreasing input level (e.g., Allen *et al.*, 1995). This correlates well with the observation that the measured DP delay regularly increases as the input levels ($a_1 = a_2$) and, therefore, the DP levels decrease (Kimberley *et al.*, 1993).

The features of the nulls that are replicated with this simple model are: (a) The null distribution of broad maxima with narrow minima shows a maximum null density which is approximately the same for the two lower-frequency DPs, $f_d(-1)$ and $f_d(-2)$. (b) The null density is the same whether f_2 is held constant, f_1 is held constant, or f_1/f_2 is held constant (Piskorski *et al.*, 1995). (c) Since, for the two higher-frequency DPs, reflections from the DP place would not reach the ear canal microphone, this model predicts that the fixed time delays for the $f_d(+2)$ and the $f_d(+3)$ DPs would not depend upon a_2/a_1 and these two higher-frequency DPs would not show nulls.

Other features in the phase data that can be explained by the model are (a) It is possible that the later wave can have more energy than the first wave, i.e., it explains the increase in the fixed time delay as a_2/a_1 exceeds a critical value. (b) It explains the commonly observed 2π bifurcations in phase upon changing level (such as shown in Fig. 7 where the phases at the two lowest input levels are different from the phases measured at the higher levels by 2π for $f_d < 2$ kHz). (c) Also, phase patterns like the one in Fig. 5 (left) are exactly what one would observe when a wave with more delay increases in relative amplitude to an early wave (as a function of the change in a_1). (d) Assuming r_{DP} increases with

decreasing amplitude of the DP, the increasing phase delay with decreasing a_1 and a_2 at constant a_2/a_1 ratio is expected.

E. Base versus apex

There seem to be differences in the DP generation mechanics when $f_2 \leqslant 1$ kHz versus when $f_2 \geqslant 2$ kHz. When $f_2 \leqslant 1$ kHz, the two lower-frequency DPs, $f_d(-1)$ and $f_d(-2)$, do not have a distinctive $f_d^{\max}$ that differs from f_2. For $f_2 \geqslant 2$ kHz, $f_d^{\max}$ is defined by a second cochlear map (Allen and Fahey, 1993). The two higher-frequency DPs, $f_d(+2)$ and $f_d(+3)$, behave in the opposite fashion. They do show a distinct $f_d^{\max}$ different from f_2 when $f_2 \leqslant 1$ kHz. When $f_2 \geqslant 2$ kHz, they do not. Some of this effect is probably due to the increasing of the input impedance Z_{in} as the frequency decreases below 1 kHz (Allen, 1986; Rosowski *et al.*, 1986). This means that, for a given value of a_1 in the ear canal, relatively less f_1 energy gets to the nonlinearity as f_1 decreases.

When $f_2 \leqslant 1$ kHz, the $f_d(+2)$ and the $f_d(+3)$ phase varies less with respect to a_1. Since low-frequency neural frequency tuning curves are less sharply tuned, the change in the DP generation properties might be due to the same mechanics that changes the low-frequency neural tuning.

Another observation that may be relevant to the difference of generation mechanics in the base versus apex is that there is broad maximum in the phase of $f_d(+2)$ and $f_d(+3)$ [see Fig. 5 (right panel) and Fig. 8] that is centered about $f_1 \approx 1$ kHz. This is a common feature in the data of the two higher-frequency DPs and it seems to be a function of f_1.

IV. SUMMARY

A. Phase observations that are a property of saturating nonlinearities

Much of the phase data discussed in this study may be explained by the basic properties of saturating nonlinearities. In Fig. 12 the phase of the $f_d(-2)$ DP is about π radians less than the phase of the $f_d(-1)$ DP over the range where phase was measured. This is also true when the phases are plotted versus f_1. In simulations we have found a phase difference of π between these two DPs to be a generic property of the saturating nonlinearities commonly used in modeling auditory phenomena. This was commented upon by Schroeder (1969) for the special case of the $f_d(-1)$ DP phase when he compared the psychophysical phase with that expected from either an expansive nonlinearity or a compressive nonlinearity and found a π phase shift that showed that the source of the $f_d(-1)$ DP is most likely due to a compressive nonlinearity. The deviations from π for successive order DPs would be a measure of the phase difference of f_1 vs f_2 at the site of the nonlinearity. A simple way to understand this is to imagine that the input/output characteristic of a saturating nonlinearity is described in terms of a power series built of odd powers only. The successive terms alternate sign. Each successive term is the dominant term in the next order DP. The change in sign leads to a change in π radians in the phase. For example, the dominant term generating the $f_d(-1)$ DP is the cubic term x^3 and the dominant term generating the $f_d(-2)$ is x^5. In a power series expansion of the input/output characteristic of a saturating nonlinearity the coefficient of x^3 is opposite in sign to the coefficient of x^5.

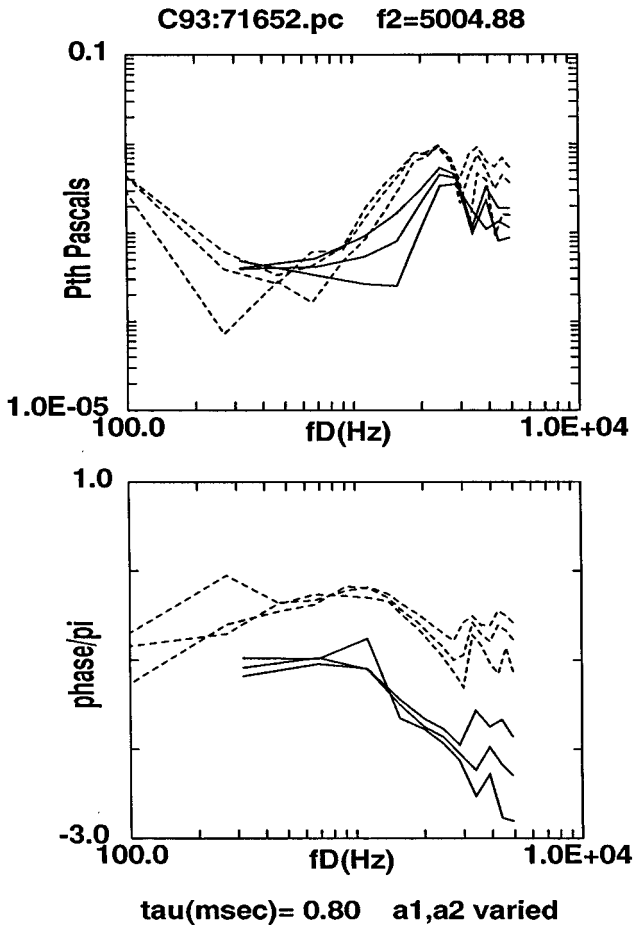

FIG. 12. The three highest magnitude and phase curves (dashed lines) are the $f_d(-1)$ DP and the three lowest (solid lines) are the $f_d(-2)$ DP. The nulls in the 3 to 4 kHz range overlap. These DPs were measured simultaneously (f_1 was decreased by the same amount for each) and, therefore, the point density in the $f_d(-2)$ DP plots is about one-half the point density in the $f_d(-1)$ plots. a_1 and a_2 are decremented together from 1.11 to 0.54 Pa. As the levels decrease the frequency of the nulls decrease and the changing pattern in the magnitude curve for the $f_d(-1)$ DP blends into the pattern for the $f_d(-2)$ DP.

The phase of a DP generated by a simple saturating nonlinearity is independent of input level(s). If it is assumed that the DP observed in the ear canal is the sum of wavelets from an ensemble of distributed saturating nonlinearities along the cochlea, and if it is assumed that the relative amplitudes of the wavelets are independent of level, then the phase of the DP measured in the ear canal would be independent of level. Observation of the magnitude and phase when a_2 is varied and is much less than $a_1 = \text{const}$ seem to fit the above assumption.

B. Phase observations explainable by two delays

For the two higher-frequency DPs [$f_d(+2)$ and $f_d(+3)$] and, under the condition that $a_2/a_1 \leqslant 2$, for the two lower-frequency DPs [$f_d(-1)$ and $f_d(-2)$] the phase has a

level independent delay that is approximately equal to $1/f_2$. It appears that the DPs are generated at the place of the higher-frequency input tone.

However, as a_2/a_1 becomes greater than 2 or 3, the delay that is measured for the two lower-frequency DPs becomes greater. This fact, combined with the observation of nulls in the amplitudes, 2π level-dependent phase bifurcations, and phase patterns such as in Fig. 5 for the two lower-frequency DPs suggest that there is a second ''source'' of the DPs that has a greater delay. We have shown that the nulls can be modeled by assuming that there is reflection of the DP from the f_d place.

ACKNOWLEDGMENTS

The authors would like to thank L. Stover and S. Neely for discussions on the filter function and the IFFT-waveform technique and to thank C. Shera and C. Talmadge for reading and helping to revise a late draft of this work.

Allen, J. B. **(1980)**. ''Cochlear micromechanics—A physical model of transduction,'' J. Acoust. Soc. Am. **68**, 1660–1670.

Allen, J. B. **(1983)**. ''Magnitude and phase frequency response to single tones in the auditory nerve,'' J. Acoust. Soc. Am. **73**, 2071–2092.

Allen, J. B. (**1986**). ''Measurement of eardrum acoustic impedance,'' in *Peripheral Auditory Mechanisms*, edited by J. B. Allen, J. L. Hall, A. Hubbard, S. T. Neely, and A. Tubis (Springer-Verlag, New York), pp. 44–51.

Allen, J. B., and Fahey, P. F. **(1992)**. ''Using acoustic distortion products to measure the cochlear amplifier gain on the basilar membrane,'' J. Acoust. Soc. Am. **92**, 178–188.

Allen, J. B., and Fahey, P. F. **(1993)**. ''A second cochlear frequency map that correlates distortion product and neural tuning measurements,'' J. Acoust. Soc. Am. **94**, 809–817.

Allen, J. B., Shaw, J., and Kimberley, B. P. (**1995**). ''Characterization of the nonlinear ear canal impedance at low sound levels,'' Abstracts of the Eighteenth Midwinter Research Meeting, Association for Research in Otolaryngology, edited by G. R. Popelka (unpublished).

Bode, H. W. (**1945**). *Network Analysis and Feedback Amplifier Design* (Van Nostrand, New York).

Born, M., and Wolf, E. (**1975**). *Principles of Optics* (Pergamon, New York), 5th ed.

Bowman, D. M., Brown, D. K., Eggermont, J. J., and Kimberley, B. P. **(1997)**. ''The effect of sound intensity in f_1-sweep and f_2-sweep distortion product otoacoustic emissions phase delay estimates in human adults,'' J. Acoust. Soc. Am. **101**, 1550–1559.

Brown, A. M., and Gaskill, S. A. (**1990**). ''Can basilar membrane tuning be inferred from distortion measurement?,'' in *The Mechanics and Biophysics of Hearing*, edited by P. Dallos, C. D. Geisler, J. W. Matthews, M. A. Ruggero, and C. R. Steele (Springer-Verlag, New York), pp. 164–169.

Brown, A. M., Gaskill, S. A., Carlyon, R. P., and Williams, D. M. **(1993a)**. ''Acoustic distortion as a measure of frequency selectivity: Relation to psychophyical equivalent rectangular bandwidth,'' J. Acoust. Soc. Am. **93**, 3291–3297.

Brown, A. M., Gaskill, S. A., and Williams, D. M. **(1992)**. ''Mechanical filtering of sound in the inner ear,'' Proc. R. Soc. London, Ser. B **250**, 29–34.

Brown, A. M., Harris, F. P., and Beveridge, H. **(1996)**. ''Two sources of acoustic distortion products from the human cochlea,'' J. Acoust. Soc. Am. **100**, 3260–3267.

Brown, A. M., Williams, D. M., and Gaskill, S. A. **(1993b)**. ''The effect of aspirin on cochlear mechanical tuning,'' J. Acoust. Soc. Am. **93**, 3298–3307.

Fahey, P. F., and Allen, J. B. **(1985)**. ''Nonlinear phenomena as observed in the ear canal and at the auditory nerve,'' J. Acoust. Soc. Am. **77**, 599–612.

Fahey, P. F., and Allen, J. B. (**1986**). ''Characterization of cubic intermodulation distortion products in the cat external auditory meatus,'' in *Peripheral Auditory Mechanisms*, edited by J. B. Allen, J. L. Hall, A. Hubbard, S. T. Neely, and A. Tubis (Springer-Verlag, New York), pp. 314–321.

Fahey, P. F., and Allen, J. B. (**1988**). ''Power law features of acoustic distortion product emissions,'' in *Basic Issues in Hearing*, edited by H. Duifhuis, J. W. Horst, and H. P. Wit (Academic, London), pp. 124–131.

He, N., and Schmiedt, R. A. **(1993)**. ''Fine structure of $2f_1-f_2$ distortion product emissions: changes with primary level,'' J. Acoust. Soc. Am. **94**, 2659–2669.

He, N., and Schmiedt, R. A. (**1996**). ''On the generation site of the fine structure of $2f_1-f_2$ acoustic distortion product in the human ear,'' Abstracts of the Nineteenth Midwinter Research Meeting, Association for Research in Otolaryngology, edited by G. R. Popelka (Association for Research in Otolaryngology, Des Moines, IA).

Hubbard, A. **(1993)**. ''A traveling-wave amplifier model of the cochlea,'' Science **259**, 68–71.

Kim, D. O., and Molnar, C. E. **(1979)**. ''A population study of cochlear nerve fibers: comparison of spatial distributions of average-rate and phase-locking measures of responses to single tone,'' J. Neurophysiol. **42**, 16–30.

Kimberley, B. P., Brown, D. K., and Eggermont, J. J. **(1993)**. ''Measuring human cochlear traveling wave delay using distortion product emission phase responses,'' J. Acoust. Soc. Am. **94**, 1343–1350.

Matthews, J. W., and Molnar, C. E. (**1986**). ''Modeling of intracochlear and ear canal distortion product $2f_1-f_2$,'' in *Peripheral Auditory Mechanisms*, edited by J. B. Allen, J. L. Hall, A. Hubbard, S. T. Neely, and A. Tubis (Springer-Verlag, New York), pp. 258–265.

O Mahoney, C. F., and Kemp, D. T. **(1995)**. ''Distortion product otoacoustic emission delay measurement in human ears,'' J. Acoust. Soc. Am. **97**, 3721–3735.

Piskorski, P., Long, G. R., Talmadge, C. L., and Tubis, A. (**1995**). ''Origin of the fine structure of the distortion product emissions in the human ear,'' Abstracts of the Eighteenth Midwinter Research Meeting, Association for Research in Otolaryngology, edited by G. R. Popelka (Association for Research in Otolaryngology, Des Moines, IA).

Rhode, W. S. **(1980)**. ''Cochlear partition vibration-recent views,'' J. Acoust. Soc. Am. **67**, 1696–1703.

Rosowski, J. J., Carney, L. H., Lynch, T. J. III, and Peake, W. T. (**1986**). ''The effectiveness of external and middle ears in coupling acoustic power into the cochlea,'' in *Peripheral Auditory Mechanisms*, edited by J. B. Allen, J. L. Hall, A. Hubbard, S. T. Neely, and A. Tubis (Springer-Verlag, New York), pp. 3–12.

Ruggero, M. A., and Rich, N. C. **(1991)**. ''Application of a commercially-manufactured Doppler-shift laser velocimeter to the measurement of basilar-membrane vibration,'' Hearing Res. **51**, 215–230.

Ruggero, M. A., Robles, L., and Rich, N. C. **(1992)**. ''Two-tone suppression in the basilar membrane of the cochlea: mechanical basis of auditory-nerve rate suppression,'' J. Neurophysiol. **68**, 1087–1099.

Schroeder, M. R. **(1969)**. ''Relation between critical bands in hearing and the phase characteristics of the cubic difference tones,'' J. Acoust. Soc. Am. **46**, 1488–1492.

Stover, L., Neely, S. T., and Gorga, M. P. **(1996)**. ''Latency and multiple sources of distortion product otoacoustic emissions,'' J. Acoust. Soc. Am. **99**, 1016–1024.

Sun, X.-M., Schmiedt, R. A., He, N., and Lam, C. F. **(1994)**. ''Modeling the fine structure of the $2f_1-f_2$ acoustic distortion product. I. Model development,'' J. Acoust. Soc. Am. **96**, 2166–2174.

Talmadge, C., Piskorski, P., Tubis, A., and Long, G. (**1996**). ''Evidence for multiple spatial origins of the fine structure of distortion product otoacoustic emissions in humans, and its implications experimental and modeling results,'' Abstracts of the Nineteenth Midwinter Research Meeting, Association for Research in Otolaryngology, edited by G. R. Popelka (Association for Research in Otolaryngology, Des Moines, IA).

Talmadge, C., Tubis, A., Piskorski, P., and Long, G. **(1995)**. ''Modeling distortion product otoacoustic emission fine structure in humans,'' J. Acoust. Soc. Am. **97**, 3413.

Voss, S. E., and Allen, J. B. **(1994)**. ''Measurement of acoustic impedance and reflectance in the human ear canal,'' J. Acoust. Soc. Am. **95**, 372–384.

Whitehead, M. L., Stagner, B. B., Lonsbury-Martin, B. L., and Martin, G. K. **(1994)**. ''Measurement of otoacoustic emissions for hearing assessment,'' IEEE Eng. Med. Biol. Mag. **13**, 210–226.

Whitehead, M. L., Stagner, B. B., Lonsbury-Martin, B. L., and Martin, G. K. **(1995)**. ''Dependence of distortion-product otoacoustic emissions on primary levels in normal and impaired ears. II. Asymmetry in L_1 and L_2 space,'' J. Acoust. Soc. Am. **97**, 2359–2377.

Whitehead, M. L., Stagner, B. B., Martin, G. K., and Lonsbury-Martin, B. L. **(1996)**. ''Visualization of the onset of distortion- product otoacoustic emissions, and measurement of their latency,'' J. Acoust. Soc. Am. **100**, 1663–1679.

Zweig, G., and Shera, C. A. **(1995)**. ''The origin of periodicity in the spectrum of evoked otoacoustic emissions,'' J. Acoust. Soc. Am. **98**, 2018–2047.

Zwicker, E. (**1981**). ''Cubic difference tone level and phase dependence on frequency and level of primaries,'' *Psychological, Physiological and Behavioral Studies in Hearing*, edited by G. van den Brink and F. A. Bilsen (Delft U.P., Delft, The Netherlands), pp. 268–273.

Zwicker, E., and Harris, F. P. **(1990)**. ''Psychoacoustical and ear canal cancellation of $(2f_1-f_2)$-distortion products,'' J. Acoust. Soc. Am. **87**, 2583–2591.